Journal of Nuclear Materials 386–388 (2009) 449–452

Contents lists available at ScienceDirect

Journal of Nuclear Materials

journal homepage: www.elsevier.com/locate/jnucmat

Microstructural characterization of Y_2O_3 ODS–Fe–Cr model alloys

V. de Castro [a,*], T. Leguey [b], A. Muñoz [b], M.A. Monge [b], R. Pareja [b], E.A. Marquis [a], S. Lozano-Perez [a], M.L. Jenkins [a]

[a] Department of Materials, University of Oxford, Oxford OX1 3PH, United Kingdom
[b] Departamento de Física, Universidad Carlos III de Madrid, 28911 Leganés, Spain

A B S T R A C T

Two Fe–12 wt% Cr alloys, one containing 0.4 wt% Y_2O_3 and the other Y_2O_3-free, have been produced by mechanical alloying followed by hot isostatic pressing. These oxide dispersion strengthened and reference alloys were characterized both in the as-HIPed state and after tempering by transmission electron microscopy and atom-probe tomography. The as-HIPed alloys exhibited the characteristic microstructure of lath martensite and contained a high density of dislocations. Small voids with sizes <10 nm were also observed. Both alloys also contained M_3C and $M_{23}C_6$ carbides (M = Cr, Fe) probably as a result of C ingress during milling. After tempering at 1023 K for 4 h the microstructures had partially recovered. In the recovered regions, martensite laths were replaced by equiaxed grains in which $M_{23}C_6$ carbides decorated the grain boundaries. In the ODS alloy nanoparticles containing Y were commonly observed within grains, although they were also present at grain boundaries and adjacent to large carbides.

1. Introduction

Reduced activation ferritic/martensitic (RAFM) steels with Cr contents ranging from 9 to 12 wt% have been proposed as candidates for use as structural materials in future fusion reactors. RAFM steels are likely to be superior to austenitic steels because of their better thermal properties and higher swelling resistance [1–3]. A major concern of these materials is their maximum service temperature, as this determines the overall efficiency of the reactor. The upper operating temperature for conventional RAFM steels is established at 550 °C. It has been demonstrated that one way to increase this temperature up to around 700 °C is to disperse homogeneously hard nanosized oxide particles, such as Y_2O_3, into the steel matrix [4]. Moreover, such nanoparticles could act as sinks for trapping of helium atoms and point defects, thus retarding radiation-induced materials degradation [5]. A promising way of fabricating oxide dispersion strengthened (ODS) steels is by mechanical alloying followed by hot isostatic pressing (HIP). This production route is recommended as an alternative to hot extrusion as it avoids strong anisotropy of the materials [6].

In Europe, efforts have focused on the ODS–RAFM–9CrW steel EUROFER. This ODS steel shows good tensile and creep properties, acceptable ductility, but poor impact properties [4,7–10]. Microstructural characterization of real steels, especially of the structures of oxide/steel matrix interfaces, which play an important role in the performance of the material, is a difficult task. In the present work we have fabricated and characterized a simpler model ODS system based on an Fe–Cr binary alloy, in the belief that this will help us better to understand complex ODS–RAFM steels. This paper reports the first microstructural characterisation of this material.

2. Experimental

Purity Fe of 99.5% and purity Cr of 99% powders with particle sizes <45 μm were mechanically alloyed at 300 rpm for 15 h under an Ar atmosphere in an Union Process vertical attrition mill. X-ray diffraction measurements confirmed the complete solution of Cr into the Fe lattice. The milling balls were made of AISI 52100 steel, and the ball to powder ratio was 20:1. For the ODS material, the alloyed powders were subsequently milled with 0.4 wt% monoclinic Y_2O_3 powder with sizes <50 nm for 12 h under the same conditions. The two batches, one containing 0.4 wt% Y_2O_3 and the other Y_2O_3-free, were canned and degassed at 623 K for 10 h in vacuum ($<10^{-1}$ Pa), and then the can was sealed. The canned powders were consolidated by HIP at 1373 K for 2 h under a pressure of 190 MPa. They were then allowed to cool at a rate of 30 K/min.

A tempering treatment at 1023 K for 4 h was applied in order to recover the microstructures. After tempering the furnace was turned off and the specimens were allowed to cool inside.

TEM samples were prepared by electropolishing 3 mm diameter disks in a TENUPOL 5 twin-jet polisher using 5% $HClO_4$ + 95% CH_3OH as electrolyte. Before each TEM session, the samples were additionally cleaned for a few minutes in an ion beam thinner at 2.5 kV. TEM characterization was carried out in a Philips CM20

* Corresponding author.
E-mail address: vanessa.decastro@materials.ox.ac.uk (V. de Castro).

0022-3115/$ - see front matter © 2009 Elsevier B.V. All rights reserved.
doi:10.1016/j.jnucmat.2008.12.136

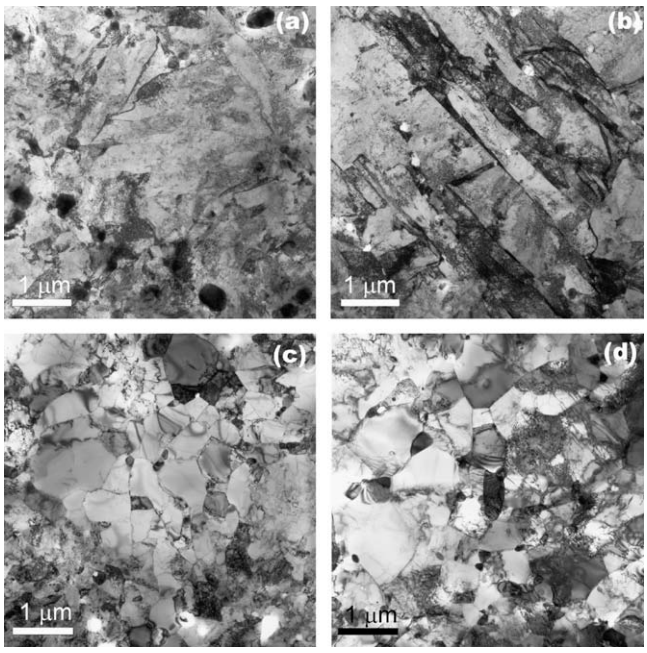

Fig. 1. Bright-field TEM images showing a general view of the ODS/Fe12Cr and reference Fe12Cr alloys: (a) as-HIPed ODS, (b) as-HIPed Fe12Cr, (c) tempered ODS, (d) tempered Fe12Cr.

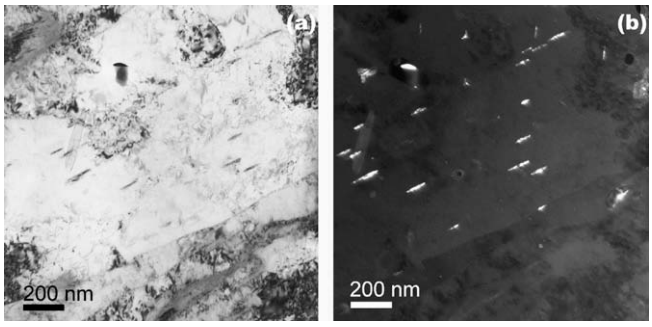

Fig. 2. Coherent carbides with needle morphology in the as-HIPed reference Fe12Cr alloy: (a) bright-field and (b) dark-field images.

equipped with an X-ray energy dispersive spectrometer (XEDS) and operated at 200 kV. HREM images, high angle annular dark-field (HAADF) images and XEDS elemental maps were obtained using a JEOL 3000F TEM operated at 300 kV.

The atom-probe tips were prepared by a standard electropolishing method [11]. Analyses were performed using a LEAP-3000X atom-probe. During analysis, the tips were held at temperature between 50 and 80 K and a pulse fraction of 20% and repetition rate of 200 kHz were used for field evaporation. IVAS software was used for data reconstruction.

3. Results and discussion

3.1. As-HIPed ODS/Fe12Cr and reference Fe12Cr alloys

Both ODS and reference as-HIPed materials presented a similar microstructure, as shown in Fig. 1(a) and (b). The grains exhibited the characteristic morphology of lath martensite with a lath width of ~100–400 nm. The martensite in the alloys is explained by the presence of ~0.09 wt% of C in the ODS material (and ~0.07 wt% in the reference sample). During the milling process, contamination from the grinding media and attritor parts is impossible to avoid, leading to C ingress. Also, a high density of dislocations was found in both alloys. This is common in steels produced by mechanical alloying and is attributed to the stresses suffered during the milling process [12].

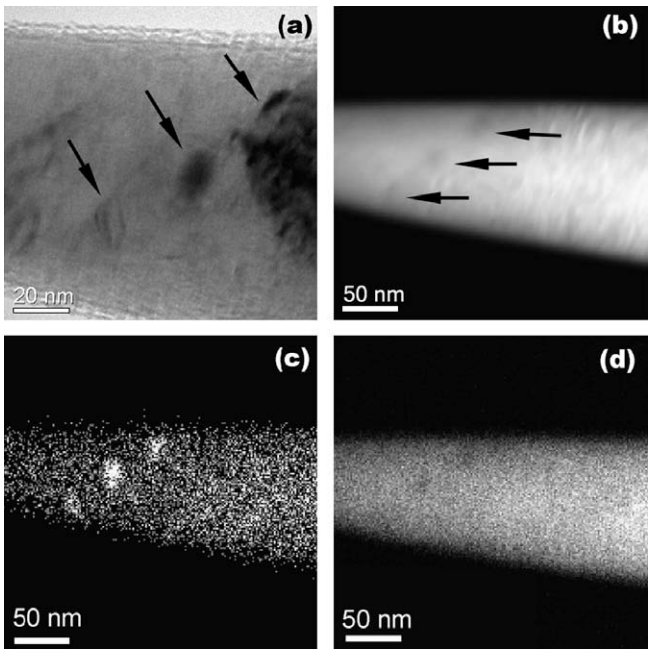

Fig. 3. TEM images showing a tip with an array of nanoparticles containing Y in the as-HIPed ODS/Fe12Cr alloy. The particles are marked with arrows. (a) Bright-field image, (b) STEM-HAADF image, (c) Elemental map showing the presence of Y in the particles, (d) Elemental map showing depletion of Fe in the particles as compared to the matrix.

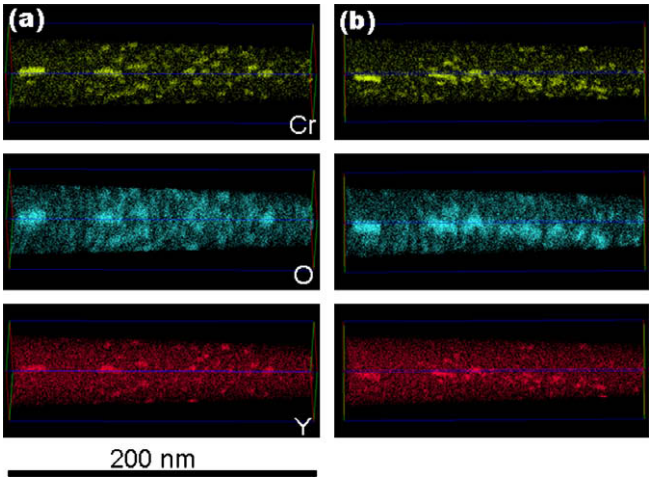

Fig. 4. (a) Atom-probe tomography reconstruction of a tip showing a dispersion of small nanoparticles containing Y, O and Cr in the as-HIPed ODS/Fe12Cr alloy. (b) Same tip rotated by 90° shows that the nanoparticles are aligned on a plane.

Two types of carbides are found in the as-HIPed alloys, with sizes up to 500 nm. XEDS spectra from coarse carbides such as those seen in Fig. 1(a) revealed a high Cr content. Selected area and convergent beam diffraction patterns from individual carbides were analyzed for different zone axes. The patterns are consistent with a face centered cubic lattice FCC. The average value for the lattice parameter is $a = (10.6 \pm 0.3)$ Å, which agrees with the reported values for $M_{23}C_6$ (M = Fe, Cr) [13]. Also, a colony of needle-shaped

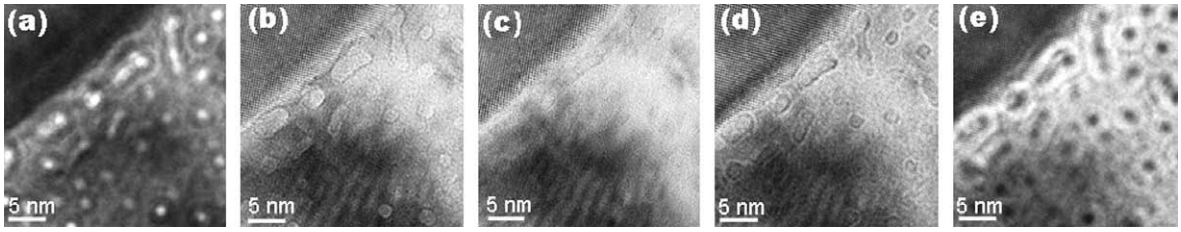

Fig. 5. HREM through-focal series of small voids adjacent to a carbide in the tempered ODS/Fe12Cr alloy. (a) Underfocused by 1 μm, (b) underfocused by 100 nm, (c) in-focus, (d) overfocused by 100 nm, (e) overfocused by 1 μm.

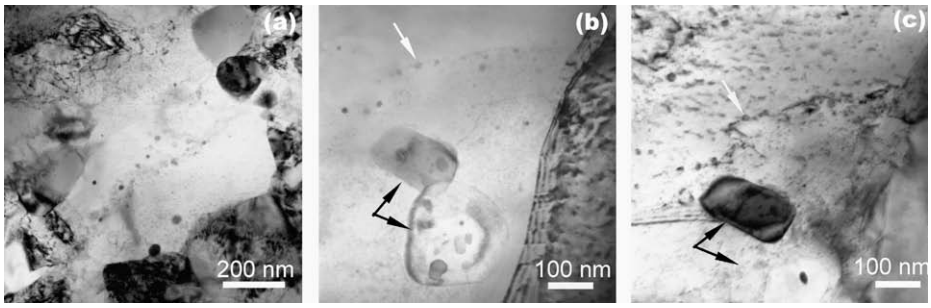

Fig. 6. Oxide nanoparticle dispersion in the tempered ODS/Fe12Cr alloy. Bright-field TEM images showing: (a) small nanoparticles inside a grain, (b) aligned nanoparticles in the matrix (white arrow) and alongside or within large carbides (black arrows), (c) same region as (b) in a different orientation reveals that the aligned nanoparticles are pinning a dislocation.

precipitates of length <100 nm was found within the martensitic grains. Dark-field images revealed that the precipitates were coherent with the matrix and tended to be distributed parallel to the long axis of the grains, see Fig. 2. Coherent cementite type carbides M_3C with similar morphology have been observed previously in steels with low carbon content [14].

For the ODS/Fe12Cr alloy, a fine dispersion of nanoparticles containing Y was found. They have sizes <50 nm, see Figs. 3 and 4. Particles were distributed in the inner region of the grains, although they were occasionally found adjacent to carbides or on grain boundaries. The TEM images in Fig. 3(a) and (b) show several nanoparticles that seem to be located along a grain boundary. Elemental maps of these particles are presented in Fig. 3(c) and (d). Nanoparticles were also found at planar defects by atom-probe tomography (APT), as shown in Fig. 4, which represents a reconstruction of an atom-probe tip showing small nanoparticles of size ~3–10 nm which contain Y, O and Cr. The same tip rotated by 90° is shown in Fig. 4(b).

Also, small voids with sizes less than 10 nm were found in both alloys and are attributed to the milling process. They were frequently observed near the ODS nanoparticles or the carbides. The presence of fine voids which could be filled with Ar gas has been recently reported in materials produced by mechanical alloying [6,15].

3.2. Tempered ODS/Fe12Cr and reference Fe12Cr alloys

The microstructures of the ODS and reference Fe12Cr alloys after tempering at 1023 K for 4 h consisted of regions of equiaxed grains of recovered ferrite with sizes up to ~1 μm, along with mainly unrecovered martensite, see Fig. 1(c) and (d). The coherent needle-shaped carbides were no longer present in the tempered alloys. During tempering of martensite at temperatures higher than ~573 K cementite carbides coarsen and subsequently transform into M_7C_3 and finally to $M_{23}C_6$ carbides, which are the ones observed in tempered ODS and reference alloys [16]. The $M_{23}C_6$ carbides had similar sizes to those seen in the as-HIPed alloys and tended to segregate to grain boundaries in the recovered regions, see Figs. 1 and 6.

Small voids were also present in the tempered alloys and were only visible when imaged out-of-focus. They appeared as white dots surrounded by a dark Fresnel fringe in underfocused images, and as dark dots surrounded by a bright Fresnel fringe in overfocused images [17]. This is illustrated in Fig. 5 which shows a through-focal series of voids located next to a $M_{23}C_6$ carbide.

The bright-field TEM images in Fig. 6 show the dispersion of ODS nanoparticles in the tempered alloys. Particles were sometimes found adjacent to $M_{23}C_6$ carbides. Line dislocations seemed strongly pinned by nanoparticles (Fig. 6(b) and (c)). Such pinning would retard the tempering process, which may explain why recovery is incomplete. XEDS spectra obtained from the particles confirm the presence of Y. No significant changes in composition were found compared to particles in the as-HIPed ODS alloy.

4. Conclusions

A model ODS system based on a Fe–12%Cr binary alloy has been produced by milling plus HIP, with the aim of simplifying the complex study of oxide nanodispersion in RAFM steels. The as-HIPed alloys presented a martensitic lath structure as a consequence of C-intake during the milling process, and a high density of dislocations. The presence of C also induced the precipitation of coarse $M_{23}C_6$ carbides and fine coherent carbides with needle morphology. An intra-granular dispersion of nanoparticles was observed in the ODS alloy, although nanoparticles were also found by carbides or on grain boundaries. Small voids with sizes <10 nm were often seen next to the ODS nanoparticles or the carbides. Tempering at 1023 K for 4 h led only to a partial recovery and recrystallization of the alloys. Pinning of dislocations by the ODS nanoparticles would retard the recovery process.

Acknowledgements

This research has been supported by FP6 Euratom Research and Training Programme on Nuclear Energy. The financial support from

the Comunidad de Madrid, through the program ESTRUMAT-CM, Grant S-0505/MAT/0077, is also gratefully acknowledged.

References

[1] D.S. Gelles, J. Nucl. Mater. 233–237 (1996) 293–298.
[2] R.L. Klueh, D.R. Harries, High Chromium Ferritic and Martensitic Steels for Nuclear Applications, American Society for Testing and Materials, West Conshohocken, PA, USA, 2001.
[3] K. Ehrlich, Fus. Eng. Des. 56&57 (2001) 71.
[4] R. Lindau, A. Möslang, M. Schirra, P. Schlossmacher, M. Klimenkov, J. Nucl. Mater. 307–311 (2002) 769.
[5] S. Ukai, M. Fujiwara, J. Nucl. Mater. 307–311 (2002) 749.
[6] Z. Oksiuta, N. Baluc, J. Nucl. Mater. (2007), doi:10.1016/j.nucmat.2007.08.004.
[7] R. Schaeublin, T. Leguey, P. Spatig, N. Balucad, M. Victoria, J. Nucl. Mater. 307–311 (2002) 778.
[8] E. Lucon, Fus. Eng. Des. 61&62 (2002) 683.
[9] C. Cayron, E. Rath, I. Chu, S. Launnois, J. Nucl. Mater. 335 (2004) 83.
[10] V. de Castro, T. Leguey, M.A. Monge, A. Muñoz, P. Fernández, A.M. Lacha, R. Pareja, J. Nucl. Mater. 367–370 (2007) 196.
[11] M.K. Miller, A. Cerezo, M.G. Hetherington, G.D.W. Smith, Atom Probe Field-Ion Microscopy, Oxford University, New York, 1996.
[12] V. de Castro, T. Leguey, M.A. Monge, A. Muñoz, R. Pareja, D.R. Amador, J.M. Torralba, M. Victoria, J. Nucl. Mater. 322 (2003) 228.
[13] A. Taylor, B.J. Kagle, Crystallographic Data on Metal and Alloy Structures, Dover Publications, New York, 1963.
[14] X. Huang, N.H. Pryds, Acta Mater. 48 (2000) 4073.
[15] M. Klimiankou, R. Lindau, A. Möslang, Micron 36 (2005) 1.
[16] H.K.D.H. Bhadesia, R.W.K. Honeycombe, Steels: Microstructure and Properties, Elsevier, 2006.
[17] M.L. Jenkins, M.A. Kirk, Characterization of Radiation damage by Transmission Electron Microscopy, Institute of Physics, 2001.